

# Nanoscale

Accepted Manuscript



This is an *Accepted Manuscript*, which has been through the Royal Society of Chemistry peer review process and has been accepted for publication.

*Accepted Manuscripts* are published online shortly after acceptance, before technical editing, formatting and proof reading. Using this free service, authors can make their results available to the community, in citable form, before we publish the edited article. We will replace this *Accepted Manuscript* with the edited and formatted *Advance Article* as soon as it is available.

You can find more information about *Accepted Manuscripts* in the [Information for Authors](#).

Please note that technical editing may introduce minor changes to the text and/or graphics, which may alter content. The journal's standard [Terms & Conditions](#) and the [Ethical guidelines](#) still apply. In no event shall the Royal Society of Chemistry be held responsible for any errors or omissions in this *Accepted Manuscript* or any consequences arising from the use of any information it contains.



## Nanoscale

## ARTICLE

## Detection of the Insulating Gap and Conductive Filament Growth Direction in Resistive Memories

E. Yalon,<sup>a</sup> I. Karpov,<sup>b</sup> V. Karpov,<sup>c</sup> I. Riess,<sup>d</sup> D. Kalav<sup>d</sup> and D. Ritter

Received 00th January 20xx,  
Accepted 00th January 20xx

DOI: 10.1039/x0xx00000x

www.rsc.org/

Filament growth is a key aspect in the operation of bipolar resistive random access memory (RRAM) devices, yet there are conflicting reports in the literature on the direction of growth of conductive filaments in valence change RRAM devices. We report here that an insulating gap between the filament and the semiconductor electrode can be detected by the metal-insulator-semiconductor bipolar transistor structure, and thus provide information on the filament growth direction. Using this technique, we show how voltage polarity and electrode chemistry control the filament growth direction during electro-forming. The experimental results and the nature of a gap between the filament and an electrode are discussed in light of possible models of filament formation.

### Introduction

There has been increasing interest in resistive switching random access memory (RRAM) technology in the past decade thanks to its potential as a highly scalable non-volatile memory<sup>1-3</sup>. In particular, oxides that show bipolar resistive switching due to the variable conduction through oxygen vacancy rich channels, often termed valence change memory (VCM), have demonstrated excellent memory performance at the device level<sup>4-6</sup>, and are therefore intensively studied<sup>1, 3, 7</sup>. It is believed that switching in these devices is governed by formation and dissolution of conductive channels, called filaments, which consist of oxygen vacancies<sup>3, 8-11</sup>. However, it is extremely challenging to obtain direct physical evidence of such filaments as well as their dimensions and shape, and characterize their electrical, thermal, and chemical properties<sup>12, 13</sup>.

The initial stage of the formation of conductive filaments by the application of voltage on the pristine device is termed electroforming (or forming). The forming process critically influences filament properties and resistive switching behaviour. Forming plays a key role in determining the polarity of the consequent (bipolar) switching<sup>14</sup>.

Conductive filaments are difficult to detect due to their nanoscale dimensions. The formation of metallic filaments in

cation-migration based resistive switching technology (electrochemical metallization - ECM) was studied and recently explained qualitatively<sup>15-19</sup>.

Observations by TEM of filaments in VCM devices are scarce<sup>12, 13</sup>, in particular observations that provide reliable information on the direction of filament growth. Consequently, a controversy regarding the filament growth direction in VCM RRAM devices is found in the literature. Several authors assume that the filament grows from the cathode side during forming<sup>12, 20-22</sup>, whereas others assume the opposite growth direction (often in different device structures)<sup>6, 23, 24</sup>. Filament growth from anode towards cathode has been reported mainly in devices with an oxygen exchange layer (OEL)<sup>24-26</sup> serving as a virtual anode. The OEL is a highly reduced layer of oxide formed between the RRAM oxide and the anode<sup>24</sup>. Fig. 1 shows a schematic illustration of the two filament growth mechanisms, described later in the text that result in opposite growth directions: (a) from cathode, and (b) from anode.

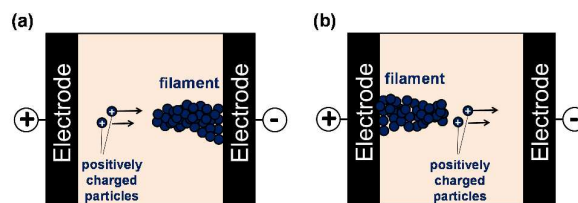


**Fig. 1** Schematic illustration of the two different growth mechanisms described in the text that result in opposite growth directions of conductive filaments in resistive memory devices: (a) from cathode, and (b) from anode. The filament consists of metal atoms in ECM and of oxygen vacancies in VCM devices. The mobile positive charges represent oxygen vacancies in VCM and metal cations in ECM. The arrows mark the direction of positively charged particles motion.

<sup>a</sup> Electrical Engineering Department, Technion – Israel Institute of Technology, Haifa 32000, Israel. E-mail: [eilamy@tx.technion.ac.il](mailto:eilamy@tx.technion.ac.il)

<sup>b</sup> Intel Corporation, Hillsboro Or. 97124, USA. E-mail: [ilya.v.karpov@intel.com](mailto:ilya.v.karpov@intel.com)

<sup>c</sup> Department of Physics and Astronomy, University of Toledo, Toledo OH 43606, USA. E-mail: [victor.karpov@utoledo.edu](mailto:victor.karpov@utoledo.edu)

<sup>d</sup> Electrical Physics, Technion – Israel Institute of Technology, Haifa 32000, Israel. E-mail: [riess@tx.technion.ac.il](mailto:riess@tx.technion.ac.il)

† Footnotes relating to the title and/or authors should appear here.

Electronic Supplementary Information (ESI) available: [details of any supplementary information available should be included here]. See DOI: 10.1039/x0xx00000x

Here, we demonstrate how the metal-insulator-semiconductor bipolar transistor can be used to detect the direction of growth of the conductive filament. The experimental results are compared with qualitative predictions of two models of filament growth dynamics. The first model is based upon the mixed ionic electronic conductor (MIEC) approach<sup>27</sup>. One dimensional simulations based upon the MIEC model suggest that the direction of filament growth in VCM devices is determined by the rate of supply of oxygen vacancies at the anode compared to the rate of their ionic motion across the oxide layer. The second model is based upon the field induced nucleation theory<sup>28</sup>, which predicts a large increase in nucleation rate due to metal electrode effects.

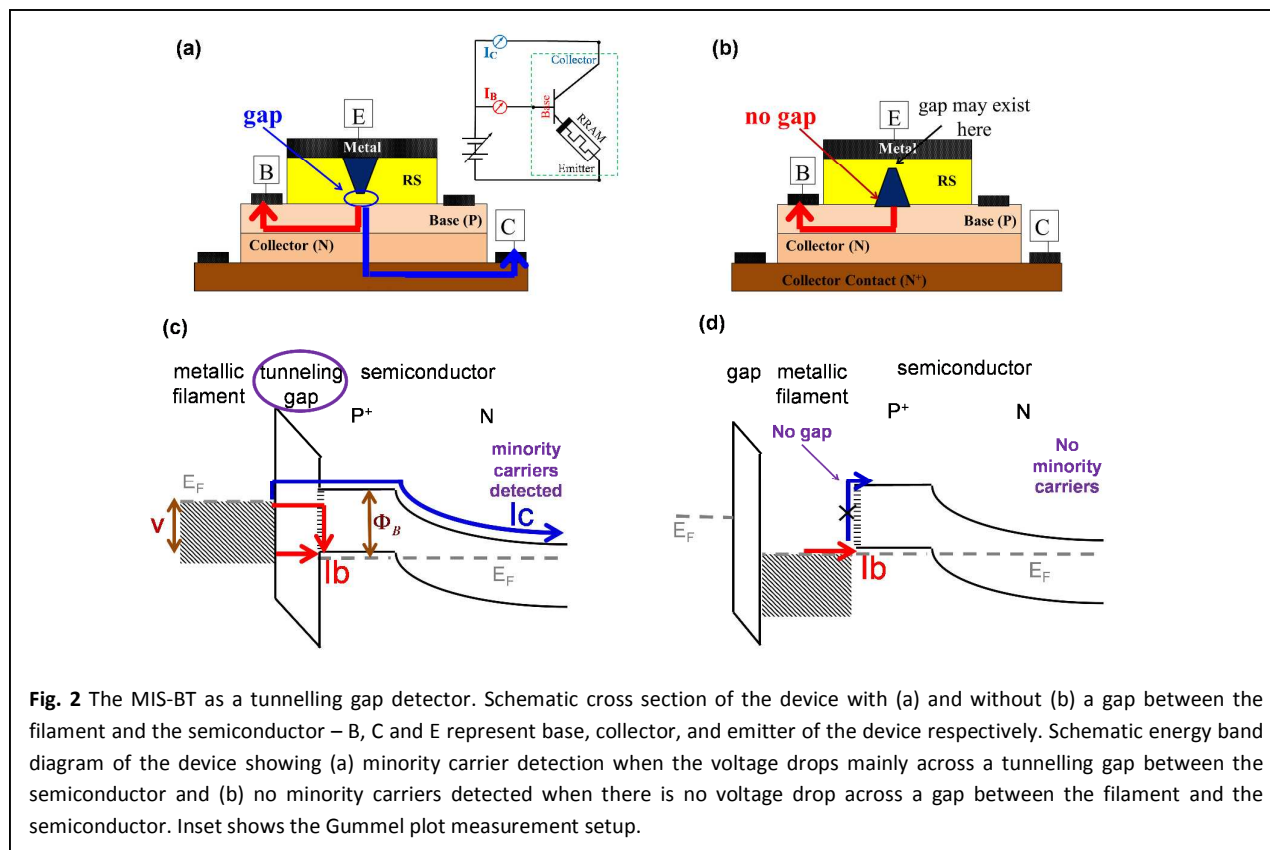
The publication is organized as follows. In section II, we describe how the metal-insulator-semiconductor bipolar transistor can be used to detect a gap between the filament and the semiconductor. Next we present the experimental results. We discuss the nature of the insulating gap in metal-insulator-metal (MIM) and metal-insulator-semiconductor (MIS) structures. We emphasize that while our technique is carried out using an MIS structure, the conclusions are relevant also for typical MIM structures.

In the last section we briefly review the two models of filament formation: the mixed-ionic-electronic-conductor model and field induced nucleation theory, and discuss the implications of the experimental results in view of these two models.

## The Device

The metal-insulator-semiconductor bipolar transistor (MIS-BT) is composed of a resistive switching material, sandwiched between a top metal electrode (the emitter) and bottom semiconductor p-n junction. The p-n junction acts as a base-collector junction of a standard bipolar transistor. The principle of operation of the device is similar to that of the tunnelling emitter bipolar transistor<sup>29-31</sup>, except that in the RRAM MIS-BT, upon electroforming of the RRAM layer, the effective emitter is the (nano-scaled) tip of the formed conductive filament<sup>21</sup>. We have previously shown that the device provides useful information on the conduction mechanism across the layer<sup>21</sup> and, more importantly, on the local filament temperature<sup>32, 33</sup>. Next, we briefly review the principle of operation of the MIS-BT to show how it can be used for detecting an insulating gap between the filament and the semiconductor<sup>34</sup>.

Fig. 2 illustrates the device. The 3-terminal Gummel plot measurement (inset of Fig. 2) is carried out as follows. The emitter (top metal) is grounded, while the base and collector are biased to the same voltage, and their currents ( $I_c$ ,  $I_b$ ) are measured separately. If an exponentially increasing collector current is detected, minority carriers are injected into the semiconductor base layer implying that: (1) a tunnelling gap exists between the filament and the semiconductor, and (2) most of the applied voltage drops across this gap (see Fig. 2). In this case, electrons are injected into the conduction band by



thermally assisted tunnelling, and the collector current is given by<sup>32</sup>:

$$I_c = S \cdot P \cdot A^* T^2 \exp\left(\frac{-q(\Phi_B - V)}{kT}\right) \quad (1)$$

where  $T$  is the temperature,  $k$  Boltzmann's constant,  $A^*$  the effective Richardson constant,  $V$  the applied voltage, and  $\Phi_B$  the potential difference between the filament Fermi level (at equilibrium) and the semiconductor conduction band, shown in Fig. 2(c). The product  $S \cdot P$  stands for the filament tip area ( $S$ ) multiplied by the tunnelling transmission probability through the barrier ( $P$ ).

If there is no gap between the filament and the semiconductor, namely when the metallic filament forms an Ohmic contact to the heavily doped semiconductor layer, only majority carriers are injected into the base, as illustrated in Fig. 2(b,d). Thus, no collector current is measured in this case. A gap may exist at the top metal side or the filament may short the top and bottom electrodes, but no collector current is measured as long as there is no gap at the semiconductor side. To conclude, the collector current is our indication for the existence of a gap between the filament and electrode: if it increases exponentially with base emitter voltage, the applied voltage drops across the gap between the filament and the semiconductor. When no collector current is detected, the applied voltage drops across the filament or some series resistance, and no gap exists between the filament and the semiconductor.

### The insulating gap

The insulating gap between the filament and one of the electrodes is central to this publication. We have previously shown that the conductive filament formed in our thin  $\text{HfO}_2$  devices is of metallic nature since it remains conductive at low temperature ( $\sim 3\text{K}$ )<sup>32</sup>. Thus, non-Ohmic conduction of our  $\text{HfO}_2$  RRAM device can only be attributed to a gap or an energy barrier between the filament and one of the electrodes. The

following section discusses the role of the insulating gap in MIM structures. Electron transport through the tunnelling gap can be modelled by tunnelling or thermally assisted tunnelling. Alternatively, it can be described as ballistic transport through a narrow constriction within the quantum point contact (QPC) model<sup>35-37</sup>.

### The insulating gap at HRS

At the HRS of a RRAM device it is natural to assume that an insulating gap exists between the conductive filament and one of the electrodes<sup>3, 14, 38-40</sup>. In bipolar devices the polarity of the applied voltage determines the direction of growth/rupture of the tip of the conductive filament, or equivalently the formation/annihilation of the gap. In unipolar or non-polar devices, on the other hand, it is also feasible that switching takes place due to variations in the radial direction.

### The insulating gap at LRS

At the LRS of a RRAM device the I-V curves are often linear, implying that conduction is Ohmic, namely a metallic filament connects the two electrodes. Nevertheless, several authors reported non-Ohmic behaviour at LRS<sup>41-43</sup>, implying that an insulating gap may also exist at the LRS<sup>40</sup>. In most cases, and in particular for filamentary RRAM devices, non-Ohmic behaviour was observed following forming at low current compliance. Fantini et al.<sup>41</sup> suggested that non-Ohmic behaviour is observed when the resistance of the conducting path is larger than the quantum resistance  $1/G_0 \approx 12.9\text{k}\Omega$ , namely the resistance of a single-mode ballistic conductor<sup>44</sup>. When a narrow constriction of the order of a few atoms impedes the current flow then the single mode conduction model applies. Fantini et al. also suggest that the value of the resistance is determined by the current compliance during the forming process<sup>41</sup>. The nature of the insulating gap at a semiconductor electrode will be discussed at the last section of this manuscript in light of the experimental results.

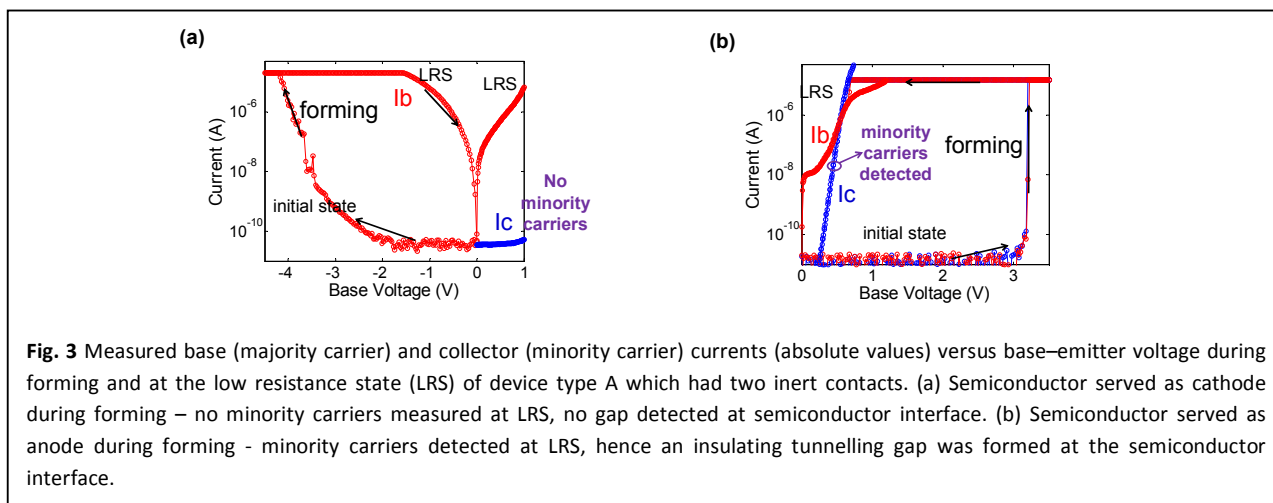


**Fig. 3** Measured base (majority carrier) and collector (minority carrier) currents (absolute values) versus base-emitter voltage during forming and at the low resistance state (LRS) of device type A which had two inert contacts. (a) Semiconductor served as cathode during forming – no minority carriers measured at LRS, no gap detected at semiconductor interface. (b) Semiconductor served as anode during forming – minority carriers detected at LRS, hence an insulating tunnelling gap was formed at the semiconductor interface.

## Experimental results

To examine the filament growth direction, two sets of MIS-BT devices were fabricated. The RRAM material was an 8 nm thick layer of  $\text{HfO}_2$  prepared by atomic layer deposition. One set of devices, referred to as type A, had two inert electrodes of high impedance to oxygen exchange: an inert top Pt electrode and an inert bottom semiconductor electrode. In the other set of devices, referred to as type B, the top electrode was composed of an oxygen exchange layer (OEL). The OEL was prepared by deposition of top Ti electrode and annealing at 400 °C in forming gas atmosphere. In addition, we prepared two control samples. The first with a top Ti electrode, but with no thermal treatment. The second control sample also had a top Ti electrode, but was subjected to the same thermal treatment before its deposition.

The InGaAs pn junction was grown by metal organic molecular beam epitaxy on n-type InP substrate. The base layer thickness was 20 nm with acceptor doping concentration of  $\sim 5 \times 10^{19} \text{ cm}^{-3}$ , and the collector was 200 nm thick unintentionally doped (donor doping concentration of  $\sim 5 \times 10^{16} \text{ cm}^{-3}$ ). The metal stack was prepared by the lift-off technique. Devices with emitter area of  $7 \times 15 \mu\text{m}^2$  and  $22 \times 45 \mu\text{m}^2$  were fabricated by standard photolithography.

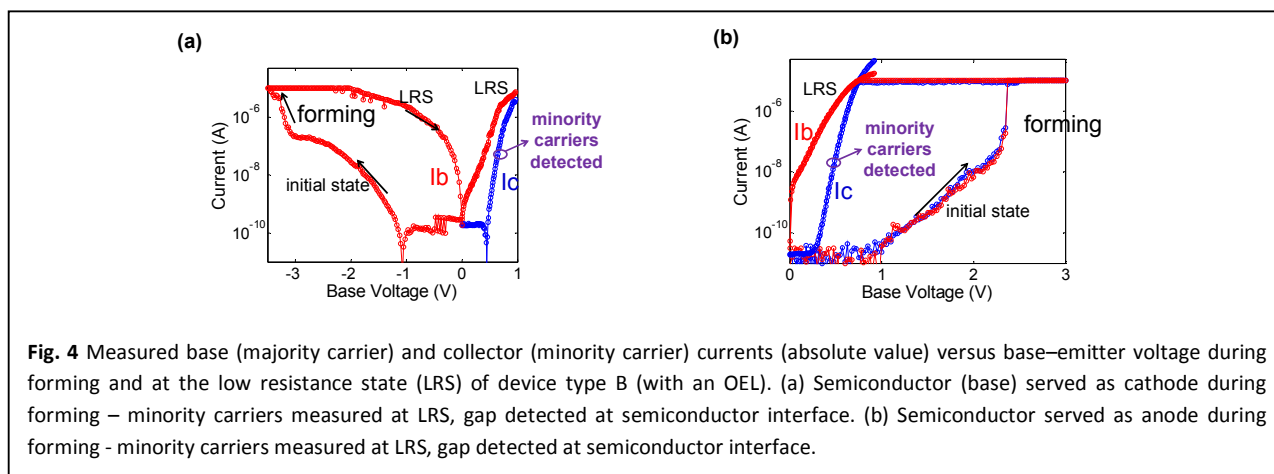
During electro-forming, the devices were divided into two groups. The first group was electro-formed at positive polarity, and the second group at negative polarity. The current compliance during electro-forming was set externally by the semiconductor parameter analyser between 10–20  $\mu\text{A}$ . Additionally, the current was limited by the serial resistance between the formed filament and the base contact (red arrow in Fig. 2a,b). The base layer sheet resistance is of the order of 1  $\text{k}\Omega/\square$ , and therefore the serial resistance between the filament and the base contact is a few  $\text{k}\Omega$ 's, depending on the filament location. The experimental results are shown in Figs. 3, 4. After forming the devices exhibit resistive switching.

Fig. 3 shows the Gummel plot characteristics of a device of type A during forming and at the low resistance state (LRS). No collector current was detected at LRS following forming by a

negative voltage applied to the semiconductor electrode. This implies that no gap existed between the filament and the semiconductor (Fig. 3a), and that the filament grew from the cathode (semiconductor electrode). A gap may have existed at the top electrode side. By contrast, an exponentially increasing collector current was obtained in devices formed by positive voltage applied to the semiconductor electrode, indicating that the filament grew from the cathode (the metal electrode) during forming (Fig. 3(b)). In summary, Fig. 3 shows that in devices with two inert (of high impedance to oxygen exchange) electrodes, the filament grew from the cathode side during forming, regardless if it was an inert metal or semiconductor electrode.

Fig. 4 presents the experimental results obtained for devices of type B, having a top OEL. In all cases, namely following forming at both polarities, an exponentially increasing collector current was obtained. Hence, a gap remained between the filament and the semiconductor after forming at both polarities, implying that the filament grew from the OEL towards the semiconductor regardless of the polarity of the forming voltage. Other scenarios, such as that the filament originated at some distance from the semiconductor electrode, are hard to justify<sup>32</sup>.

Our interpretation of the experimental results is illustrated in Fig. 5, which shows the forming process of type A and B devices at the two different polarities. When both electrodes are of high impedance to oxygen exchange, the filament grows from the cathode side. However, when the anode is an OEL, the filament grows from the anode. In the next section we discuss our finding within the MIEC model, and within the field induced nucleation model. We point out that the number of set/reset cycles in our devices is limited due to the sensitivity of the semiconductor pn junction to the high current density and heating in the vicinity of the filament. We therefore limit this report to include forming and LRS characteristics. We finally mention, that both control samples (described above) showed the same behaviour as the devices having top Pt electrode (type A), implying that the difference in growth directions between devices type A and B is due to the OEL, rather than changes in the bulk oxide caused by thermal



**Fig. 4** Measured base (majority carrier) and collector (minority carrier) currents (absolute value) versus base–emitter voltage during forming and at the low resistance state (LRS) of device type B (with an OEL). (a) Semiconductor (base) served as cathode during forming – minority carriers measured at LRS, gap detected at semiconductor interface. (b) Semiconductor served as anode during forming – minority carriers measured at LRS, gap detected at semiconductor interface.

treatment.

### The insulating gap at a semiconductor electrode

If one of the RRAM electrodes is a semiconductor, as in the device described in this publication, the filament to electrode contact at LRS is essentially a metal-semiconductor contact. Typical contact resistance of the metal/p-InGaAs system at a doping concentration of  $p=5 \cdot 10^{19} \text{ cm}^{-3}$ , as in our experiment, is of the order of  $\rho_c \sim 10 \Omega \cdot \mu\text{m}^2$ <sup>45,46</sup>. Hence, when the filament grows from the metal electrode towards the semiconductor, and the filament tip diameter is of the order 1-10 nm<sup>21,32</sup>, the contact resistance of the filaments is  $10^5$ - $10^7 \Omega$ . In this case, most of the applied voltage drops across the filament semiconductor contact, and the small area Ohmic contact between the filament and the semiconductor is practically equivalent to a tunnelling gap. On the other hand, when the filament grows from the semiconductor towards the metal contact, the diameter of the filament at the semiconductor may be much larger. In this case, the voltage drop across the filament semiconductor contact is small, and no minority carrier current is detected. In the schematic illustrations shown in Fig. 5a, with the left inert electrode representing the semiconductor electrode in our device, the filament may also connect between the two electrodes with the narrow tip at the anode side.

The material filling the insulating gap in RRAM devices may either be composed of the pristine insulator, e.g. HfO<sub>2</sub> in our devices, or an oxide of the electrode. The electrode-oxide can be formed either during device fabrication or during electroforming. If one of the electrodes is a semiconductor, it is expected that a thin oxide of the semiconductor constituting elements will be present, as is the case for the MIS-BT devices described in this publication.

### Models of Filament Growth

Two different models can help understand the experimentally observed effect of the OEL layer on the filament growth direction. These two complementary models are described in this Section.

#### Mixed ionic electronic conduction

The MIEC approach attempts to solve the coupled ionic and electronic continuity equations. A simple 1D simulation was recently described in<sup>27</sup>, where a single mobile ionic defect (positively charged oxygen vacancies which act as donors) and a single type of negative charge carriers, namely the free electrons in the conduction band, were considered. A uniform low concentration of oxygen vacancies was assumed in the pristine device. The temperature was uniform (though higher than room temperature). The vacancy distribution induced by an applied voltage (the forming process) was calculated in<sup>2</sup>

for different types of ion and electron kinetics at the bulk and electrodes. It was shown that the direction of the conductive

region growth is determined by the relation between the ion kinetics at the electrode and that of the bulk. Qualitatively, the positively charged donors are attracted towards the cathode, where they accumulate and form a conductive region, unless they are supplied at such a high rate that their concentration in the vicinity of the anode is sufficient to initiate the formation of a conductive region there, followed by its propagation towards the cathode. The simulations carried out in<sup>27</sup> thus predict that during electro-forming, formation of the conductive region starts from the cathode when electrode kinetics (rate of oxygen vacancy supply) are limited in comparison to the fast kinetics of oxygen vacancies in the bulk. In the opposite case, which is achieved experimentally by introducing an OEL at the anode, the conductive region forms from the anode.

This above model predictions motivated this study, and were confirmed by the experimental results shown in Fig. 5. We note that since the positively charged oxygen vacancies drift towards the cathode, the OEL must serve as the anode during forming in order to affect the kinetics of filament formation. Indeed, devices having an OEL at the anode exhibited superior RRAM characteristics<sup>4,6,23-25</sup>.

MIEC model is capable of explaining the existence of an insulating gap between the filament and one of the electrodes. According to the MIEC model, when the anode is of high impedance to material exchange with the ambient, positively charged oxygen vacancies drift towards the cathode, while there is no supply of vacancies from the anode. Thus, a region depleted of oxygen vacancies must be formed at the anode, as demonstrated in Fig. 5(a,b).

#### Field induced nucleation switching

The field induced nucleation (FIN) concept<sup>47-50</sup> first developed for phase change memory<sup>28</sup>, describes how it can be energetically favourable to form a conductive needle shaped nucleus in an insulating material under strong enough electric field  $E$ . The FIN approach is based upon a thermodynamic model, where the free energy gain is of electrostatic nature: it is given by the energy  $F_E = p \cdot E$  of the strong electric dipole  $p = \alpha \cdot E$  induced in the conductive embryo of length  $h$  having the polarizability  $\alpha = h^3$ . The FIN concept does not depend on the details of system structure and is equally applicable to phase change memory and resistive memory systems; it can as well explain dielectric breakdown in thin insulating films. Experimental evidence for FIN was observed in several PCM devices<sup>50</sup>, and filamentary RRAM devices<sup>51,52</sup>. Note that the FIN model complements the MIEC model as it describes filament formation from the thermodynamic point of view regardless of its chemical composition.

Assuming the dominance of the electrostatic energy gain, the FIN model predicts the time to form a conductive filament at the electrode<sup>28</sup>:

$$\tau = \tau_0 \exp\left(\frac{W_0 E^2}{kTV}\right) \quad (2)$$

where  $\tau_0$  and  $\bar{V}$  are material parameters,  $kT$  is the thermal energy, and  $V$  is the voltage across the insulating layer. It is straightforward that adding to the electrostatic energy a small contribution from the difference  $\mu$  in chemical potentials per volume between the conducting and insulating phases, leads to the renormalization:

$$\bar{V} \rightarrow \bar{V} \left[ 1 + \frac{\pi}{3} \frac{\mu}{\epsilon E^2} \left( \frac{1}{2} \frac{d}{h} \right)^2 \right] \quad (3)$$

where  $d/h \ll 1$  is the small ratio of the filament diameter over its height, and  $\epsilon$  is the electric permittivity.

The chemical potential correction is relevant here because it helps understand the role of positive vacancy saturation in the case of Fig. 5a, when the filament forms at the cathode owing the local environment overcrowded with oxygen vacancies. That phenomenon immediately follows from the latter two equations where  $\mu$  linearly decreases with the vacancy concentration. In fact, these equations offer a possible experimental verification via measuring the devices using different switching fields where the effect of vacancy concentration is predicted to be different.

In the present context, the chemical potential correction predicts the observation of filament formation at the OEL regardless of the voltage polarity. One other useful prediction of FIN model is based on the recently found effect of the nucleation barrier decrease due to the image charges related to a metal electrode<sup>47</sup>: it follows that the filament forms on the electrode and not in the middle of the device.

The FIN model also provides explanation to the formation of a gap between the filament tip and the electrode. It is based on the separation between the regimes of constant charge vs. that of constant potential across the capacitor forming the RRAM structure. The overlay between these regimes takes place when the filament growth time,  $t$ , is comparable to the RC

time of the system. When  $RC \gg t$ , the system is recharging and slowly maintaining the condition of constant charge  $Q$ . Correspondingly, the electrostatic energy  $Q^2/2C$  decreases when its capacitance increases as the filament grows. The condition  $RC \ll t$  corresponds to fast recharging and constant voltage regime, for which the electrostatic energy  $CV^2/2$  increases with capacitance as the filament grows. Therefore, in this regime the filament growth becomes energetically unfavourable leaving a gap between the tip and the electrode. We have verified that the RC parameter in the low resistance and high resistance states takes values that are respectively smaller and greater than the characteristic time of filament formation, in accordance with the above prediction.

The validity of this model requires that the electro-static energy is dominant, namely heating is insignificant, and the gap maintains its dielectric properties during the set/forming process. We have measured our devices using low current compliance of 10  $\mu\text{A}$  and built in based resistor which reduce self-heating effects. We speculate that in devices that show an Ohmic behaviour in the LRS (i.e. no gap exists), significant self-heating occurs during the forming process.

## Conclusions

In this work, we provided experimental evidence for the filament growth direction in VCM RRAM. We have shown that the metal-insulator-semiconductor bipolar transistor structure is useful as a detector for the existence of a gap between the filament and a semiconductor electrode, and therefore provides instrumental information on the filament growth dynamics. Furthermore, our experimental technique shows how to control the filament growth direction during forming by varying polarity and electrode chemistry. The experimental results are analyzed and in agreement with two different models describing the filament formation: one based upon mixed-ionic-electronic-conduction, and the other based on field induced nucleation. Additionally, the nature of the insulating gap in bipolar RRAM devices of both metal-insulator-semiconductor (MIS) and metal-insulator-metal (MIM) structures was discussed.

## Acknowledgements

This work was supported by the Semiconductor Research Corporation (SRC) task # 2437.001. I. Riess acknowledges support of Israel Science Foundation Grant No. 699/11. E. Yalon gratefully acknowledges the support of The Clore Israel Foundation Scholars Programme and the Russel Berrie Nanotechnology Institute, Technion.

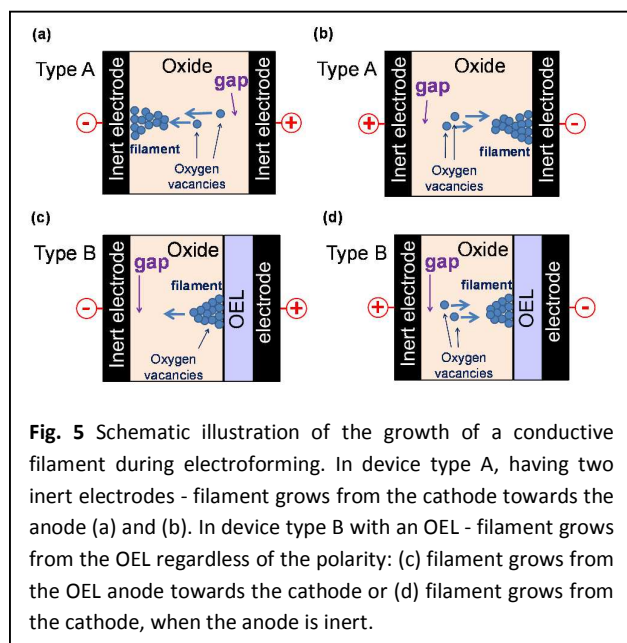


**Fig. 5** Schematic illustration of the growth of a conductive filament during electroforming. In device type A, having two inert electrodes - filament grows from the cathode towards the anode (a) and (b). In device type B with an OEL - filament grows from the OEL regardless of the polarity: (c) filament grows from the OEL anode towards the cathode or (d) filament grows from the cathode, when the anode is inert.

## References

- 1 H. Akinaga and H. Shima, *Proc IEEE*, 2010, 98, 2237-2251.
- 2 D. S. Jeong, R. Thomas, R. Katiyar, J. Scott, H. Kohlstedt, A. Petraru and C. S. Hwang, *Reports on Progress in Physics*, 2012, 75, 076502.
- 3 H. S. Wong, H. Lee, S. Yu, Y. Chen, Y. Wu, P. Chen, B. Lee, F. T. Chen and M. Tsai, *Proc IEEE*, 2012, 100, 1951-1970.
- 4 B. Govoreanu, G. Kar, Y. Chen, V. Paraschiv, S. Kubicek, A. Fantini, I. Radu, L. Goux, S. Clima and R. Degraeve, *10×10nm<sup>2</sup> Hf/HfOx crossbar resistive RAM with excellent performance, reliability and low-energy operation*, *IEEE Int. Electron Devices Meet. Tech. Dig.*, 2011.
- 5 A. C. Torrezan, J. P. Strachan, G. Medeiros-Ribeiro and R. S. Williams, *Nanotechnology*, 2011, 22, 485203.
- 6 M. J. Lee, C. B. Lee, D. Lee, S. R. Lee, M. Chang, J. H. Hur, Y. B. Kim, C. J. Kim, D. H. Seo and S. Seo, *Nature Materials*, 2011, 10, 625-630.
- 7 J. J. Yang, D. B. Strukov and D. R. Stewart, *Nature Nanotechnology*, 2012, 8, 13-24.
- 8 R. Waser, *Microelectronic Engineering*, 2009, 86, 1925-1928.
- 9 R. Waser and M. Aono, *Nature materials*, 2007, 6, 833-840.
- 10 D. B. Strukov, J. L. Borghetti and R. S. Williams, *small*, 2009, 5, 1058-1063.
- 11 S. Larentis, F. Nardi, S. Balatti, D. C. Gilmer and D. Ielmini, *Electron Devices, IEEE Transactions on*, 2012, 59, 2468-2475.
- 12 D. Kwon, K. M. Kim, J. H. Jang, J. M. Jeon, M. H. Lee, G. H. Kim, X. Li, G. Park, B. Lee and S. Han, *Nature nanotechnology*, 2010, 5, 148-153.
- 13 G. Park, Y. B. Kim, S. Y. Park, X. S. Li, S. Heo, M. Lee, M. Chang, J. H. Kwon, M. Kim and U. Chung, *Nature communications*, 2013, 4.
- 14 R. Waser, R. Dittmann, G. Staikov and K. Szot, *Adv Mater*, 2009, 21, 2632-2663.
- 15 Y. Yang, P. Gao, L. Li, X. Pan, S. Tappertzhofen, S. Choi, R. Waser, I. Valov and W. D. Lu, *Nature communications*, 2014, 5.
- 16 Y. Yang and W. Lu, *Nanoscale*, 2013, 5, 10076-10092.
- 17 Y. Yang, P. Gao, S. Gaba, T. Chang, X. Pan and W. Lu, *Nature communications*, 2012, 3, 732.
- 18 S. Qin, J. Zhang and Z. Yu, *A unified model of metallic filament growth dynamics for conductive-bridge random access memory (CBRAM)*, *IEEE Int. Conf. on Simulation of Semiconductor Processes and Devices (SISPAD)*, 2013.
- 19 S. Menzel, S. Tappertzhofen, R. Waser and I. Valov, *Physical Chemistry Chemical Physics*, 2013, 15, 6945-6952.
- 20 X. Guan, S. Yu and H. S. Wong, *Electron Devices, IEEE Transactions on*, 2012, 59, 1172-1182.
- 21 E. Yalon, A. Gavrilov, S. Cohen, D. Mistelev, B. Meyler, J. Salzman and D. Ritter, *Electron Device Letters, IEEE*, 2012, 1-3.
- 22 V. Havel, A. Marchewka, S. Menzel, S. Hoffmann-Eifert, G. Roth and R. Waser, *Electroforming of Fe: STO samples for resistive switching made visible by electrocoloration observed by high resolution optical microscopy*, Cambridge Univ Press, 2014.
- 23 G. Bersuker, D. Gilmer, D. Veksler, J. Yum, H. Park, S. Lian, L. Vandelli, A. Padovani, L. Larcher and K. McKenna, *Metal oxide RRAM switching mechanism based on conductive filament microscopic properties*, *IEEE Int. Electron Devices Meet. Tech. Dig.*, 2010.
- 24 D. Gilmer, G. Bersuker, S. Kovesnikov, M. Jo, A. Kalantarian, B. Butcher, R. Geer, Y. Nishi, P. Kirsch and R. Jammy, *Asymmetry, vacancy engineering and mechanism for bipolar RRAM*, *IEEE Int. Memory Workshop*, 2012.
- 25 H. Lee, P. Chen, T. Wu, Y. Chen, C. Wang, P. Tzeng, C. Lin, F. Chen, C. Lien and M. Tsai, *Low power and high speed bipolar switching with a thin reactive Ti buffer layer in robust HfO<sub>2</sub> based RRAM*, *IEEE Int. Electron Devices Meet. Tech. Dig.*, 2008.
- 26 A. Padovani, L. Larcher, P. Padovani, C. Cagli and B. De Salvo, *Understanding the role of the Ti metal electrode on the forming of HfO<sub>2</sub>-based RRAMs*, *IEEE Int. Memory Workshop*, 2012.
- 27 D. Kalaev, E. Yalon and I. Riess, *Solid State Ionics*, 2015, 276, 9-17.
- 28 V. Karpov, Y. Kryukov, I. Karpov and M. Mitra, *Physical Review B*, 2008, 78, 052201.
- 29 H. Kasaki, *Proc IEEE*, 1973, 61, 1053-1054.
- 30 J. Xu and M. Shur, *IEEE Electron Device Lett.*, 1986, 7, 416-418.
- 31 E. Aderstedt, I. Medugorac and P. Lundgren, *Solid-State Electronics*, 2002, 46, 497-500.
- 32 E. Yalon, S. Cohen, A. Gavrilov and D. Ritter, *Nanotechnology*, 2012, 23, 465201.
- 33 E. Yalon, A. A. Sharma, M. Skowronski, J. A. Bain, D. Ritter and I. V. Karpov, *Electron Devices, IEEE Transactions on*, 2015.
- 34 E. Yalon, D. Kalaev, I. Riess and D. Ritter, *Detection of the conductive filament growth direction in resistive memories*, *IEEE 72<sup>nd</sup> Annu. Dev. Research Conf.*, 2014.
- 35 X. Lian, S. Long, C. Cagli, J. Buckley, E. Miranda, M. Liu and J. Suñé, *Quantum point contact model of filamentary conduction in resistive switching memories*, *IEEE 13<sup>th</sup> Int. Conf. on Ultimate Integration on Si (ULIS)*, 2012.
- 36 E. A. Miranda, C. Walczyk, C. Wenger and T. Schroeder, *Electron Device Letters, IEEE*, 2010, 31, 609-611.
- 37 R. Degraeve, A. Fantini, S. Clima, B. Govoreanu, L. Goux, Y. Y. Chen, D. Wouters, P. Roussel, G. S. Kar and G. Pourtois, *Dynamic 'hour glass' model for SET and RESET in HfO<sub>2</sub> RRAM*, *IEEE Symp. on VLSI Tech. (VLSIT)*, 2012.
- 38 M. D. Pickett, D. B. Strukov, J. L. Borghetti, J. J. Yang, G. S. Snider, D. R. Stewart and R. S. Williams, *J. Appl. Phys.*, 2009, 106, 074508-074508-6.
- 39 A. Sawa, *Materials Today*, 2008, 11, 28-36.
- 40 S. Menzel, U. Böttger and R. Waser, *J. Appl. Phys.*, 2012, 111, 014501.
- 41 A. Fantini, D. Wouters, R. Degraeve, L. Goux, L. Pantisano, G. Kar, Y. Chen, B. Govoreanu, J. Kittl and L. Altimime, *Intrinsic switching behavior in HfO<sub>2</sub> RRAM by fast electrical measurements on novel 2R test structures*, *IEEE Int. Memory Workshop*, 2012.
- 42 F. Lentz, B. Roesgen, V. Rana, D. J. Wouters and R. Waser, *Electron Device Letters, IEEE*, 2013, 34, 996-998.
- 43 F. Miao, J. P. Strachan, J. J. Yang, M. Zhang, I. Goldfarb, A. C. Torrezan, P. Eschbach, R. D. Kelley, G. Medeiros-Ribeiro and R. S. Williams, *Adv Mater*, 2011, 23, 5633-5640.
- 44 S. Datta, *Electronic transport in mesoscopic systems*, Cambridge university press, 1997.
- 45 M. J. Rodwell, M. Le and B. Brar, *Proc IEEE*, 2008, 96, 271-286.
- 46 E. Yalon, D. Cohen Elias, A. Gavrilov, S. Cohen, R. Halevy and D. Ritter, *IEEE Electron Device Lett.*, 2011, 32, 21-23.
- 47 V. Karpov, R. Maltby, I. Karpov and E. Yalon, *Phys. Rev. Applied*, 2015, 3, 044004.
- 48 V. Karpov, Y. Kryukov, S. Savransky and I. Karpov, *Appl. Phys. Lett.*, 2007, 90, 123504.
- 49 M. Nardone, V. G. Karpov, D. C. S. Jackson and I. V. Karpov, *Appl. Phys. Lett.*, 2009, 94, 103509 (DOI:10.1063/1.3100779).
- 50 I. V. Karpov, M. Mitra, D. Kau, G. Spadini, Y. A. Kryukov and V. G. Karpov, *Appl. Phys. Lett.*, 2008, 92, 173501 (DOI:10.1063/1.2917583).
- 51 I. Valov and G. Staikov, *Journal of Solid State Electrochemistry*, 2013, 17, 365-371.
- 52 P. Gomon, M. Mougnot, C. Vallée, C. Jorel, V. Jousseume, H. Grampeix and F. El Kamel, *J. Appl. Phys.*, 2010, 107, 074507.